

## An Iterative Method for the Construction of Equilibrium $N$ -Body Models for Stellar Disks

S.A. Rodionov (seger@astro.spbu.ru)

N.Ya. Sotnikova (nsot@astro.spbu.ru)

*Sobolev Astronomical Institute, St. Petersburg State University, St. Petersburg*

One widely used technique for the construction of equilibrium models of stellar disks is based on the Jeans equations and the moments of velocity distribution functions derived using these equations. Stellar disks constructed using this technique are shown to be “not entirely” in equilibrium. Our attempt to abandon the epicyclic approximation and the approximation of infinite isothermal layers, which are commonly adopted in this technique, failed to improve the situation substantially. We conclude that the main drawback of techniques based on the Jeans equations is that the system of equations employed is not closed, and therefore requires adopting an essentially *ad hoc* additional closure condition. A new iterative approach to constructing equilibrium  $N$ -body models with a given density distribution is proposed. The main idea behind this approach is that a model is first constructed using some approximation method, and is then allowed to adjust to an equilibrium state with the specified density and the required parameters of the velocity distribution remaining fixed in the process. This iterative approach was used to construct isotropic, spherically symmetric models and models of stellar disks embedded in an external potential. The numerical models constructed prove to be close to equilibrium. It is shown that the commonly adopted assumption that the profile of the radial velocity dispersion is exponential may be wrong. The technique proposed can be applied to a wide range of problems involving the construction of models of stellar systems with various geometries.

arXiv:astro-ph/0611176v1 6 Nov 2006

# 1 Introduction

In studies of the dynamic evolution of galaxies using the results of numerical  $N$ -body simulations, it is very important to correctly specify the initial equilibrium state of the stellar system. Two different approaches are employed to achieve this. The first approach uses the kinetic equation (collisionless Boltzmann equation) and the second approach deals with the equations of stellar hydrodynamics (Jeans equations). Both approaches have their advantages and disadvantages.

The kinetic approach is based on the use of the phase-space distribution function (DF) and the Jeans theorem, which states that any function of integrals of the motion is a solution of the stationary collisionless Boltzmann equation [1]. For spherically symmetric stellar systems with isotropic velocity distributions, any function of the form  $f(E)$ , where  $E$  is the specific energy, describes an equilibrium gravitating system. If spherically symmetric models with a density distribution profile  $\rho(r)$  that corresponds to the observational data and a potential  $\Phi(r)$  derived from the Poisson equation are applied to real objects (elliptical galaxies and various subsystems of spiral galaxies, such as the bulge and halo), determining the distribution function  $f(E)$  reduces to solving an integral equation derived via the Abel transform (Eddington's formula; see e.g., [1]). Analytical solutions of this equation are known only for special classes of models<sup>1</sup>. Researchers often prefer a different approach, proceeding from a particular form of  $f(E)$  and integrating it over velocity space to obtain the density distribution and then the potential. One can then choose from among the broad class of analytical models constructed in this way those whose density profiles are closest to the density profile of the real system.

The transition to anisotropic or axisymmetric models, e.g., stellar-disk models, drastically complicates the problem. Describing a disk system requires the use of a distribution function of the form  $f(E, L_z)$ , where  $L_z$  is the angular momentum of a particle with respect to the symmetry axis  $z$ . A number of models are known to have analytical formulas simultaneously for  $f(E, L_z)$ ,  $\rho$ , and  $\Phi$  (simple models include the Kalnajs [5] disk, however, this is not the only one). Such models can be used to study the properties of flat systems only as a first approximation. These are usually 2D models and their radial profiles usually differ strongly from the exponential form typical of spiral galaxy disks.

As for 3D axisymmetric models, constructing such models using the distribution function  $f(E, L_z)$  also faces another serious barrier. In systems represented by such distribution functions, the radial velocity dispersion should be equal to the velocity dispersion parallel to the rotation axis (see, e.g., [1]), which is inconsistent with observational data – at least with data for our Galaxy based on measurements of stellar velocity dispersion in the solar neighborhood (see, e.g., [6]). In the kinetic approach, axisymmetric models with anisotropic radial and vertical velocity distributions can be represented by a function of the form  $f(E, L_z, I_3)$ , where  $I_3$  is the third integral of the motion. The general expression for  $I_3$  is unknown. In sufficiently cool stellar disks, where the stellar velocity dispersion is small compared to the velocity of the disk's rotation about the symmetry axis, the energy of vertical oscillations  $E_z = \Phi(R, z) - \Phi(R, 0) + \frac{1}{2}v_z^2$  is a well-conserved quantity (along almost circular orbits). This can be used as a third integral of motion when constructing

---

<sup>1</sup>For example, the distribution function corresponding to the popular dark halo model – the Navarro-Frenk-White [2] model – can be determined only numerically [3], [4].

the DF for thin stellar disks with density distributions  $\rho_{\text{disk}}(R, z)$ , close to the observed exponential law [7], [8]. Kuijken and Dubinski [7] and Widrow and Dubinski [8] also describe a procedure for correcting the DF in the case of multicomponent galaxy models. These authors actually solve a more general problem – the construction of the distribution function for a disk-galaxy model consisting of several self-consistently components: an exponential disk, bulge, dark halo, etc. However, even more specific problems, such as a construction of an equilibrium model for a disk with a realistic density profile, which is embedded in the external potential, is not easy to produce as an initial configuration for  $N$ -body simulations.

The second approach, which is based on computing the moments of the equilibrium particle velocity distribution function, uses the Jeans equations. In the case of constructing equilibrium stellar-disk models with realistic density profiles, this approach usually consists of various modifications of the technique described by Hernquist [9].

This technique has the advantage that it is relatively simple and makes it possible to construct a model that is more or less close to equilibrium for a given density distribution profile  $\rho_{\text{disk}}(R, z)$  and external potential  $\Phi_{\text{ext}}(R, z)$ , under reasonable assumptions about the velocity distribution function. However, this technique has an important drawback: the resulting  $N$ -body model is often far from equilibrium. This primarily concerns models with small masses for the spheroidal components (bulge and halo). We analyze the technique of Hernquist in more detail in the next section.

In this paper, we offer a new iterative method for constructing equilibrium models of stellar disks embedded in an external (rigid) potential, which we compare to the widely used method based on the moments of the distribution function. Our iterative models are very close to equilibrium and have the specified density profile. The iterative approach has a broader scope than the particular problem we are solving, and can be used to both construct models with a different geometry (e.g., spherically symmetric models with a given mass distribution and anisotropy of the random motions) and construct equilibrium models of selfconsistent multicomponent stellar systems.

## 2 Approach based on the moments of the distribution function

If a stellar disk with density  $\rho_{\text{disk}}(R, z)$  and an external potential  $\Phi_{\text{ext}}(R, z)$  produced, e.g., by the halo and bulge, are axisymmetric, the Jeans equations for the first and second moments of the velocity distribution function for the disk particles can be written in the form [1], [10]

$$\left\{ \begin{array}{l} \bar{v}_\varphi^2 = v_c^2 + \sigma_R^2 - \sigma_\varphi^2 + \frac{R}{\rho_{\text{disk}}} \frac{\partial(\rho_{\text{disk}}\sigma_R^2)}{\partial R}, \\ \sigma_\varphi^2 = \frac{\sigma_R^2 R}{2\bar{v}_\varphi} \left( \frac{\partial\bar{v}_\varphi}{\partial R} + \frac{\bar{v}_\varphi}{R} \right), \\ \frac{\partial(\rho_{\text{disk}}\sigma_z^2)}{\partial z} = -\rho_{\text{disk}} \frac{\partial\Phi_{\text{tot}}}{\partial z}, \end{array} \right. \quad (1)$$

where  $\bar{v}_\varphi$  is the mean azimuthal velocity<sup>2</sup>;  $\sigma_R$ ,  $\sigma_\varphi$ , and  $\sigma_z$  are the velocity dispersions in the radial, azimuthal, and vertical directions, respectively<sup>3</sup>;  $\Phi_{\text{tot}} = \Phi_{\text{ext}} + \Phi_{\text{disk}}$  is the total potential produced by all components of the system; and  $v_c = R \frac{\partial \Phi_{\text{tot}}}{\partial R}$  is the circular velocity. Here, we have omitted the dependences of parameters on the coordinates  $R$  and  $z$  in the cylindrical coordinate system for simplicity.

Equations (1) assume the absence of regular motions in the radial and vertical directions. We also assume that the axes of the velocity ellipsoid are directed along the axes of the cylindrical coordinate system; this means that second moments of the form  $\overline{v_R v_z}$  are equal to zero. This is a reasonable assumption for the galactic plane (based on symmetry considerations). However, outside the galactic plane, the velocity dispersion ellipsoid is inclined [10], so that the equality  $\overline{v_R v_z} = 0$  breaks down, although substantial deviations appear only in the central regions of the disk.

The system (1) consists of three equations and has four unknowns:  $\bar{v}_\varphi$ ,  $\sigma_R$ ,  $\sigma_\varphi$ , and  $\sigma_z$ . To solve such a system, one should make some additional assumption, and this is the major drawback of methods of constructing equilibrium models for stellar disks based on the Jeans equations.

One of the most popular techniques for constructing equilibrium (or, more precisely, close-to-equilibrium)  $N$ -body stellar-disk models based on the Jeans equations is described by Hernquist [9]. Many authors (see, e.g., [11], [12], [13], [14], [15]) have applied this technique with various minor modifications. It is usually applied to three-dimensional disks with exponential density profiles:

$$\rho_{\text{disk}}(R, z) = \begin{cases} \frac{M_{\text{disk}}}{4\pi h^2 z_0} \exp\left(-\frac{R}{h}\right) \text{sech}^2\left(\frac{z}{z_0}\right) & , R \leq R_{\text{max}} , \\ 0 & , R > R_{\text{max}} . \end{cases} \quad (2)$$

Here,  $h$  is the exponential disk scale,  $z_0$  is the vertical scale length,  $M_{\text{disk}}$  is the total mass of the disk<sup>4</sup>, and  $R_{\text{max}}$  the disk radius (truncation radius). This density profile approximates well the observed profiles of real spiral galaxies [16].

Further, the conditions under which the Jeans equations (1) were derived should be supplemented with the following additional assumptions [9].

1. All four moments ( $\bar{v}_\varphi$ ,  $\sigma_R$ ,  $\sigma_\varphi$ , and  $\sigma_z$ ) are independent of  $z$  and depend only on the cylindrical radius  $R$ ; i.e., the disk is isothermal in the  $z$  direction.
2. The epicyclic approximation is valid (random velocities of stars are small compared to the velocity of rotation). In this case, the mean azimuthal velocity in the second equation of (1) can be replaced by the circular velocity (i.e., we can substitute  $v_c$  for  $\bar{v}_\varphi$ ).
3. The last equation of (1) is often rewritten in the approximation of infinitesimal isothermal layers [17]. In this case, the contribution of the external potential to

---

<sup>2</sup>An overline denotes averaging.

<sup>3</sup>In accordance with the usual astronomical usage, the dispersion denotes the standard deviations of the distribution function.

<sup>4</sup>Formally,  $M_{\text{disk}}$  is the total mass of the disk at  $R_{\text{max}} = \infty$ .

the total potential  $\Phi_{\text{tot}}$  is often neglected. This yields the relation  $\sigma_z^2 = \pi G \Sigma_{\text{disk}} z_0$ , where  $\Sigma_{\text{disk}}$  is the surface density of the disk.

4. The velocity distribution function has the Schwarzschild form, i.e., the velocity components along each of the three axes of the cylindrical coordinate have normal distributions.

These are standard assumptions, are believed to be appropriate for real galaxies [1].

The system (1) is closed under the additional assumptions:  $\sigma_R^2 \propto \exp(-R/h)$ . It is convenient to specify the coefficient of proportionality via the Toomre parameter  $Q_{\text{T}}$  [18] at some radius  $R_{\text{ref}}$ . This parameter characterizes the degree of disk heating, or the margin of stability against the growth of perturbations in the disk plane. For a stellar disk with an exponential density profile in  $R$ , the relation  $\sigma_R^2 \propto \exp(-R/h)$  means that  $\sigma_R^2$  is proportional to the surface density  $\Sigma_{\text{disk}}$ . Together with the isothermal layer approximation, this also yields a dependence of the form  $\sigma_R \propto \sigma_z$ . Observational data for our Galaxy [19], [20] are consistent with the dependence  $\sigma_R^2 \propto \exp(-R/h)$ . It is believed from general considerations that this relations is also appropriate to other spiral galaxies [21]. We examine the validity of this assumption below.

As a result, one can construct for a given  $\rho_{\text{disk}}$  and  $\Phi_{\text{ext}}$  a one parametric family of models parametrized by a quantity that characterizes the degree of disk heating, or the fraction of the kinetic energy of the disk contained in random motions.

The deficiency of this approach is that the constructed stellar disks prove to be not entirely in equilibrium. Although the models rapidly adjust to equilibrium, this adjustment may complicate analyses of the results of  $N$ -body simulations, such as those used to study instabilities of the stellar disk. In the process of this adjustment, a characteristic ringlike density wave forms and propagates from the center, as is illustrated by the results of our numerical simulations<sup>5</sup> in Fig. 1 (see [14], [15] for a more detailed description of the technique used for the numerical simulations). Kuijken and Dubinski [7] also pointed out a similar effect. The most nonequilibrium models are hot models (with large  $Q_{\text{T}}(R_{\text{ref}}) \approx 2$ ) and models without halos or with low mass halos. The only nearly equilibrium models are those with fairly massive halos (such as the models described by Hernquist [9], where the mass of the halo within four exponential disk scales was greater than five disk masses).

The nonequilibrium nature of the models constructed using the Hernquist technique is due to the underlying assumptions of this technique. Our attempt to refine this approach by abandoning the epicyclic and isothermal layer approximations did not result in any substantial improvement of the models.

For example, the solution of the equation of vertical equilibrium (the third equation of (1)) and of the equation derived from it in the isothermal layer approximation yield similar  $\sigma_z(R, z)$  in many cases, and have little effect on the extent to which the models are nonequilibrium. The results of the ensuing computations illustrate this conclusion. Since the equation of vertical equilibrium contains only one unknown,  $\sigma_z$ , when  $\rho(R, z)$

---

<sup>5</sup>In all numerical simulations that used stellar-disk model (2), we set  $G = 1$ ,  $h = 3.5$ , and  $M_{\text{disk}} = 1$ . If needed, the results of our simulations can be interpreted in a dimensional system of units (one of several possible) in which the unit of length is  $R_u = 1$  kpc and the unit of mass is  $M_u = 8 \cdot 10^{10} M_{\odot}$ . The units of time and velocity are then  $t_u \approx 1.67$  Myr and  $v_u \approx 587$  km/s.

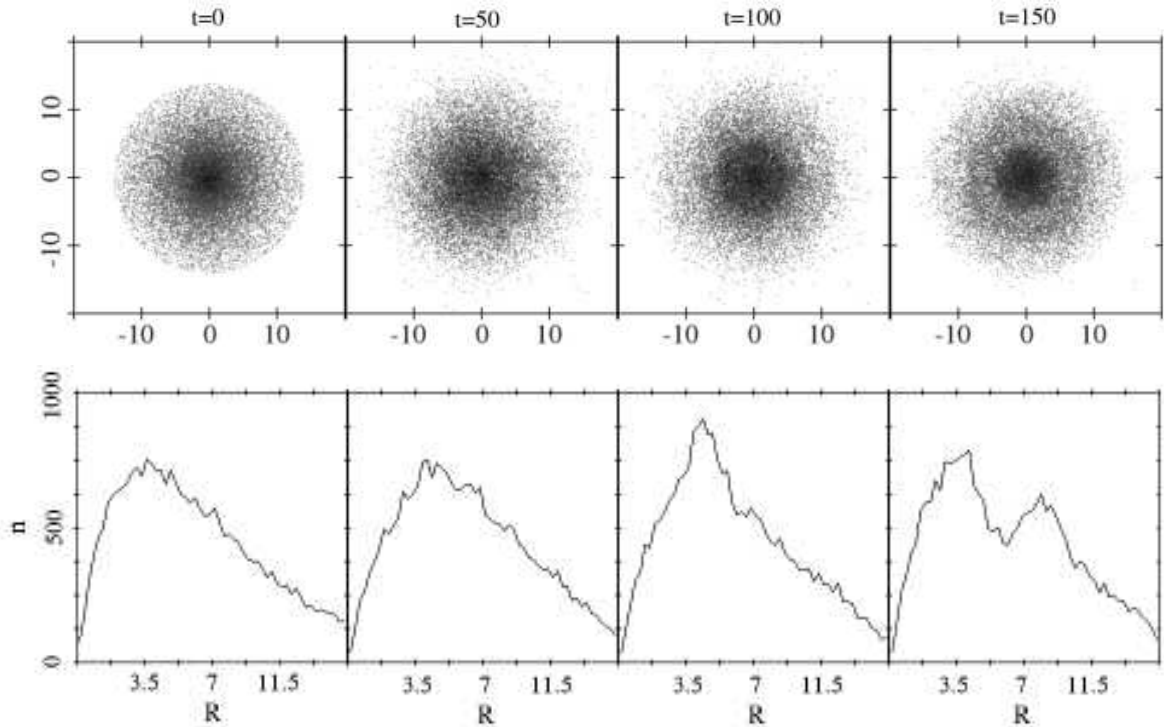


Figure 1: Adjustment to equilibrium of the model constructed using the Hernquist technique (see Section 2). The top snapshots show a face-on view for several times, with the shades of gray corresponding to the logarithm of the particle number per pixel. The plots at the bottom show the radial distribution of the number of particles (counts made in concentric cylindrical layers). A characteristic wave propagating from the center can be seen. The exponential disk model (2) is used with parameters  $h = 3.5$ ,  $z_0 = 1$ ,  $M_{\text{disk}} = 1$ , and  $R_{\text{max}} = 14$ . The external potential has the form of a Plummer sphere (4) with  $a_{\text{pl}} = 15$  and  $M_{\text{pl}} = 4$ . For these parameters, the total fractional mass of the spherical component within four exponential disk scales is about 1.3 (i.e.,  $M_{\text{sph}}(4h)/M_{\text{disk}}(4h) \approx 1.3$ ). The Toomre parameter is  $Q_{\text{T}}(R_{\text{ref}}) = 1.5$ , where  $R_{\text{ref}} = 8.5$ . 150 time units approximately corresponds to one disk rotation period at  $R = 8.5$ . The number of particles, smoothing parameter, and integration step are  $N = 25000$ ,  $\epsilon = 0.02$ , and  $dt = 0.01$ , respectively.

is specified, this equation can be solved independently of the other equations<sup>6</sup>. As is evident from Fig. 2, the approximation of infinite isothermal layers breaks down only if the external potential in the system is represented by a very massive dark halo (the “disk + heavy halo” curves) or varies strongly over a vertical disk scale height, e.g., when the system has a bulge (the “disk + bulge” curves). If the system has no external potential at all (the “disk” curves) or is represented by a small halo with a mass comparable to the mass of the disk (the “disk + light halo” curves), then the two methods yield virtually the same dispersion (except for the centermost regions, where the approximation of infinite isothermal layers obviously breaks down, although, even there, the differences are not very large).

We believe that the nonequilibrium state of the models is due primarily to the adopted additional assumption concerning the dependence of  $\sigma_R$  on  $R$ .

Note that a number of authors have adopted other assumptions, different from the proportionality  $\sigma_R^2 \propto \exp(-R/h)$ , or equivalently  $\sigma_R \propto \sigma_z$ , as the missing equation in the system of Jeans equations. For example, Athanassoula and Misiriotis [13] adopted the additional assumption that the Toomre parameter  $Q_T$  is independent of radius. Revaz and Pfenniger [11] assumed that  $\sigma_R \propto \sigma_z \frac{\nu}{\kappa}$ , where  $\kappa$  is the epicyclic frequency and  $\nu$  is the frequency of the vertical oscillations, ( $\nu^2 = \frac{\partial^2 \Phi_{\text{tot}}}{\partial z^2}$ ). They computed the coefficient of proportionality as in the original technique of Hernquist, by specifying the Toomre parameter at some radius.

So far, we have no grounds to prefer any particular additional condition to supplement the Jeans equations. However, by taking into account all the moments up to the sixth inclusive, and if that all the moments beginning with the second are small compared to the circular velocity, this problem can be solved without invoking additional assumptions [23], [24]. Unfortunately, due to its complexity and awkwardness, this solution has never been used to construct  $N$ -body models of stellar disks.

### 3 Dependence of the radial velocity dispersion on the cylindrical radius (dependence of $\sigma_R$ on $R$ )

The assumption that  $\sigma_R \propto \sigma_z$  is now generally accepted, or, in any case, it is used to analyze and interpret the observation data [21], [25], [26]. However, is this assumption justified?

Thus far, the observed dependence of  $\sigma_R$  on  $R$  has been obtained only for the Milky Way. Based on a derivation of this dependence from observations of K giants, Lewis and Freeman [19] concluded that  $\sigma_R^2 \propto \exp(-R/h)$ . In the isothermal layer approximation, this means that  $\sigma_R \propto \sigma_z$ . However, we must emphasize an important point. The errors in

---

<sup>6</sup>For example, Revaz and Pfenniger [11], Khoperskov et al. [12], and Bahcall [22] used the solution of this equation in analyses of the equilibrium in the vertical direction and the construction of equilibrium models for stellar disks. Note that this equation can be solved in two ways. As we did here, one can specify the density profile and find  $\sigma_z(R, z)$ . Alternatively,  $\sigma_z(R, z)$  can be specified – for example, by assuming that  $\sigma_z$  is independent of  $z$  [22] – in order to determine the vertical density profile. Khoperskov et al. [12] implemented the latter approach.

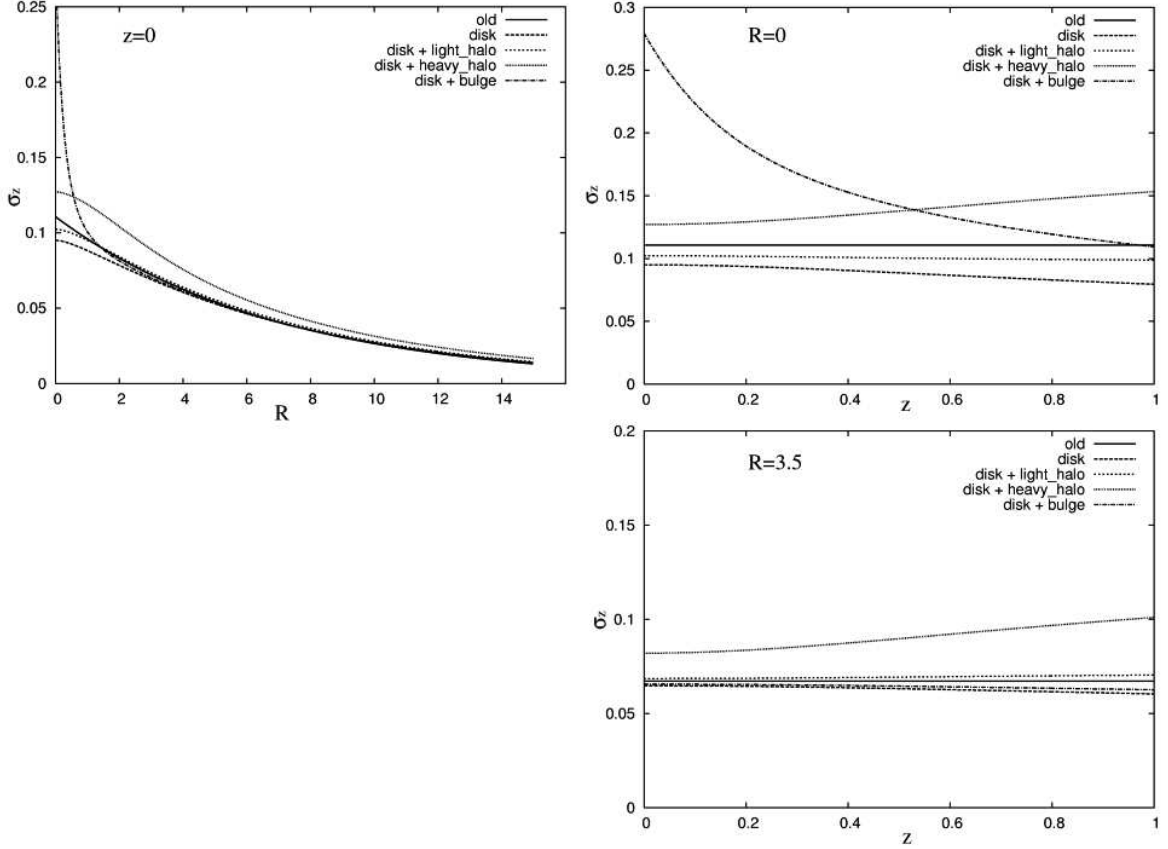


Figure 2: Dispersion of the vertical stellar velocities,  $\sigma_z$ , computed both in the approximation of infinite isothermal layers and without this approximation for various external potentials. The top left plot shows the computed dispersion in the disk plane ( $z = 0$ ), the top right plot the dependence of the dispersion on  $z$  at  $R = 0$ , and the bottom right plot the dependence of the dispersion on  $z$  at  $R = 3.5$ . In this case, we used a model of a relatively thin exponential disk (2) with  $h = 3.5$ ,  $z_0 = 0.3$ ,  $M_{\text{disk}} = 1$ , and  $R_{\text{max}} = \infty$ . The “old” curve shows the dispersion computed in the approximation of infinite isothermal layers. All other curves were constructed without this assumption and the corresponding models differ in the adopted external potentials: the “disk” model was computed with no external potential, the “disk + light halo” model with an external potential in the form of Plummer sphere (4) with  $a_{\text{pl}} = 3.5$  and  $M_{\text{pl}} = 1$ , the “disk + heavy halo” curve with an external potential in the form of the Plummer sphere with  $a_{\text{pl}} = 3.5$  and  $M_{\text{pl}} = 5$ , and the “disk + bulge” curve with an external potential in the form of a Hernquist (9) sphere with  $a_{\text{hr}} = 0.5$  and  $M_{\text{hr}} = 0.1$ .

the dispersion obtained by Lewis and Freeman [19] are fairly large (on the order of 10%), as are the errors in the stellar distances, which were derived indirectly. Accurate (errors of the order of one percent) measurements of  $\sigma_R$  are available only in the solar neighborhood, based on HIPPARCOS data [6]. Therefore, for the Galaxy, we can only conclude that  $\sigma_R$  is approximately proportional to  $\sigma_z$ . It seems possible that, if the dependence of  $\sigma_\varphi$  on  $R$  for the Galaxy could be measured with the same accuracy as we now know the dependence for  $\sigma_R$ , it would also fit the relation  $\sigma_\varphi \propto \exp(-R/2h) \propto \sigma_z$ . This situation should improve when new astrometric satellites (in particular, GAIA) are launched. At least for the Galaxy, the dependence of the moments of the velocity distribution function on  $R$  will then be known more accurately.

It is not possible to obtain  $\sigma_R(R)$  for other galaxies directly from observations, which can yield only the line-of-sight velocity,  $v_{\text{los}}$ , and line-of-sight velocity dispersion,  $\sigma_{\text{los}}$ . For edge-on galaxies,  $\sigma_{\text{los}}$  depends on both  $\sigma_R$  and  $\sigma_\varphi$ , whereas, for intermediate-inclination galaxies, all three components of random velocities ( $\sigma_R$ ,  $\sigma_\varphi$ ,  $\sigma_z$ ) contribute to  $\sigma_{\text{los}}$ . However, we can use the Jeans equations (1) to derive the unknown dependence  $\sigma_R$  on  $R$  from the observed quantities  $v_{\text{los}}$  and  $\sigma_{\text{los}}$ . Gerssen et al. [27], [26], Shapiro et al. [28], and Wefallet al. [29] used such considerations to infer the velocity dispersions in three directions from observational data for inclined galaxies. The drawback of the technique they used is that it involves an a priori assumption about the form of the dependence of  $\sigma_R$  and  $\sigma_z$  on  $R$ :

$$\begin{aligned}\sigma_z(R) &= \sigma_{z,0} \exp(-R/a), \\ \sigma_R(R) &= \sigma_{R,0} \exp(-R/a),\end{aligned}\tag{3}$$

where  $a$ ,  $\sigma_{z,0}$ , and  $\sigma_{R,0}$ , are parameters determined during the reduction of the data. These authors pointed out that there are no grounds to believe that the scale parameter  $a$  should be the same for  $\sigma_z$  and  $\sigma_R$ , but the quality of the observational data prevents independent determination of these two scale parameters.

It follows that the quality of the observational data available so far prevents the determination of the dependence of  $\sigma_R$  on  $R$  for external galaxies, and available observations can only yield estimates of the velocity dispersion for the entire galaxy.

We also note the two semi-theoretical papers [30] and [31], whose authors used independent methods to conclude that  $\sigma_R \propto \sigma_z$  is not valid for our Galaxy.

## 4 Iterative method for constructing equilibrium models

$N$ -body simulations sometimes use the following method to specify the initial conditions. The initial conditions are specified (in some way) to be close to equilibrium. The system is then given some time to adjust to a new equilibrium state, which is used as the initial state for the  $N$ -body simulations (Sellwood and Athanassoula [32] and Barnes [33] used this approach with some modifications). The drawback of this technique is that it is difficult to build a close-to-equilibrium model with a given density profile.

We developed a method that is essentially a logical extension of the above technique. The main idea of our method is to allow the system to adjust to the equilibrium state

while fixing the density profile. We achieve this via the following general algorithm for the iterative method.

1. Use some approximate method to construct a close-to-equilibrium  $N$ -body model with a given density distribution (i.e., with a given particle distribution function in space)<sup>7</sup>.
2. Allow the model to evolve for a short time.
3. Construct a model with the same velocity distribution as that of the evolved model, but with the required density profile (the initial density profile). Note that, if we have certain constraints on the particle velocity distribution (e.g., if we want to construct a Plummer sphere model with an isotropic velocity distribution), we must correct the particle velocity distribution to satisfy these constraints.
4. Return to item 2. Stop iterations when the velocity distribution ceases to change.

As a result, we obtain a close-to-equilibrium  $N$ -body model with the given density profile.

Practical implementation of the iterative method is somewhat more difficult. The main problem arises at the third stage – the construction of a model with the same velocity distribution as for the slightly evolved model of the previous iteration step. In the ideal case, we would have to obtain the particle velocity distribution at each point of the system. This is, naturally, impossible, given the available number of particles in the  $N$ -body simulation. However, this problem can be resolved if we make some simplifying assumptions.

The next section describes how an iterative method can be used to construct a spherically symmetric, equilibrium, isotropic model with a given distribution function (a Plummer sphere). In the problem at hand, this enables us to verify that the iterative method indeed permits the construction of an equilibrium model. This realization of the technique can be used to construct spherically symmetric, isotropic-velocity models with other density profiles and, with small modifications, even models with anisotropic velocity distributions. Below we apply the iterative method to construct equilibrium  $N$ -body models for stellar disks. The realization of the third part of the algorithm in the case of spherically symmetric models differs from that for disk models, but the main idea remains the same.

## 4.1 Equilibrium, isotropic, spherically symmetric models

To test the idea of the iterative method, we will use it to construct an equilibrium model for a case when the equilibrium distribution function is known a priori: an equilibrium, isotropic model of a Plummer sphere. The isotropy means that there is no special direction in velocity space, i.e., the velocity distribution function depends only on the speed. The

---

<sup>7</sup>This initial model does not have to be close to equilibrium. In the next section, we use a cold model (with zero velocities) as an initial approximation to construct an equilibrium Plummer sphere.

equilibrium distribution function for this model is known (see, e.g., [1], p. 223), and the potential for this model has the form

$$\Phi_{\text{pl}}(r) = -\frac{GM_{\text{pl}}}{(r^2 + a_{\text{pl}}^2)^{1/2}}, \quad (4)$$

where  $M_{\text{pl}}$  is the total mass for the model and  $a_{\text{pl}}$  is the scale length (the Plummer model has about 35% of its mass inside the radius  $a_{\text{pl}}$ ).

We now implement the third part of the algorithm of the iterative method (the “transfer” of the velocity distribution function) as follows. We take our slightly evolved model, from which we plan to copy the velocity distribution function. We subdivide this model into spherical layers containing approximately the same number of particles and construct the distribution of the particle speeds  $v$  in each of these spherical layers.

We do this in the usual way, by determining the range of variation of  $v$  and subdividing this interval into some number of bins. We then compute the number of particles falling in each bin. In the limit of an infinite number of particles and infinite number of bins, the resulting histogram gives the distribution function (not normalized to unity). We assumed that the number of particles in a bin is equal to the value of distribution function at the center of the bin. We can then approximate these values by some function and use this as the distribution function. We used several types of approximation: piecewise-linear, cubic spline, and least-squares fits using functions of the form  $\exp(P(x))$ , where  $P(x)$  is a polynomial. The type of fit had virtually no effect on the result of the iterative algorithm.

This yields the distribution function of velocity modulus in each of the spherical layers. We then constructed the model for the next iteration step as follows. We specified the positions of the particles in accordance with the given density profile. We then determined the spherical layer to which each particle belongs, and used the “selection-rejection” method with the distribution function for the given spherical layer to determine the speed, choosing the direction for the velocity as random.

The velocity distribution function for the new model is isotropic and spherically symmetric (here, we mean that the velocity distribution function is symmetric in coordinate space<sup>8</sup>). We did not simply transfer the velocity distribution function, but adjusted it to make it strictly isotropic and spherically symmetric.

We now apply the algorithm described above to construct an equilibrium model for the Plummer sphere. We use virial units ( $G = 1$ , the total mass of the model is  $M_{\text{pl}} = 1$ , and the total energy is  $E = -1/4$ ). In iterative models, we truncated the density distribution at  $r_{\text{max}} = 5$  (the sphere of this radius contains about 98% of the mass of the modeled system).

Let us consider two models constructed using iterative method:

- model “li” with a piecewise-linear approximation for the distribution function;
- model “epol,” in which the distribution function is approximated by functions of the form  $\exp(P(x))$ , where  $P(x)$  is a polynomial (we used a sixth-degree polynomial).

---

<sup>8</sup>Isotropy can be considered to be spherical symmetry in velocity space.

We constructed both models in 120 iterations, with the first 100 having relatively low accuracy. The number of particles is  $N = 10^5$ , the number of spherical layers used to subdivide the system  $n_r = 50$ , and the number of bins used to construct the distribution function of the speed  $v$  in each spherical layers,  $n_v = 21$ . We performed the last 20 iterations with relatively high accuracy:  $N = 5 \cdot 10^5$ ,  $n_r = 200$ ,  $n_v = 31$ . The time step for each iteration is  $t_i = 1$  (which approximately corresponds to the crossing time of the system’s core in the adopted units). Our starting point was a cold model with zero velocities.

Note that the initial model in our computations is far from equilibrium; however, the iterations converge to close-to-equilibrium models. Figure 3 demonstrates the convergence of the iterations during the construction of model li. It is clear that the iterations converge to the equilibrium model. Departures from equilibrium are evident only at the periphery of the system. For example, the velocity dispersion,  $\sigma_v$ , for model li differs appreciably from the value given by the equilibrium model at  $r > 3$  (Fig. 3). However, the system has only about 5% of its mass located outside the sphere of radius  $r = 3$ .

Let us now experimentally test the equilibrium of our models by comparing them with two other models. The first one is constructed using the equilibrium distribution function as an example of the closest-to-equilibrium model (model “DF”), and the second is constructed using another approximation method, based on the following main idea. We can compute the mean speeds,  $\bar{v}$ , and velocity dispersion,  $\sigma_v$ , at each radius of the equilibrium model for the Plummer sphere:

$$\begin{aligned}\bar{v} &\approx 0.665\sqrt{-\Phi_{\text{pl}}(r)}, \\ \sigma_v &\approx 0.240\sqrt{-\Phi_{\text{pl}}(r)}.\end{aligned}\tag{5}$$

The numerical coefficients in (5) are determined in virial units by integrating the equilibrium distribution function (in virial units,  $M_{\text{pl}} = 1$  and  $a_{\text{pl}} = 3\pi/16$ ).

An approximate model can be constructed assuming that the speed distribution function is Gaussian with the moments (5); we will call this as the “gauss” model.

Let us compare the initial stages of the evolution of the four  $N$ -body models for the Plummer sphere (li, epol, DF, and gauss) for  $N = 50\,000$ . We chose the integration step and smoothing parameter for the potential  $\epsilon$  in  $N$ -body simulations in accordance with the recommendations derived in [34] ( $dt = 0.002$ ,  $\epsilon = 0.007$ ).

We analyzed the results using the  $\Delta_r$  and  $\Delta_v$  values introduced and determined as follows (we used similar quantities in our earlier paper [34]).

The quantity  $\Delta_r$  characterizes the spatial deviation of the particles at time  $t$  from the initial distribution (at time  $t = 0$ ). We computed this by subdividing the model into spherical layers, computing in each spherical layer the difference between the numbers of particles at time  $t$  and at the initial time, and then computing  $\Delta_r$  as the sum of the absolute values of these differences, normalized to the total number  $N$  of particles in the system. The thickness of the layer and maximum radius were 0.1 and 2, respectively.

Note the very important point that the value of  $\Delta_r$  for two random realizations of any model is not zero. This quantity has appreciable natural noise due to the finite number of

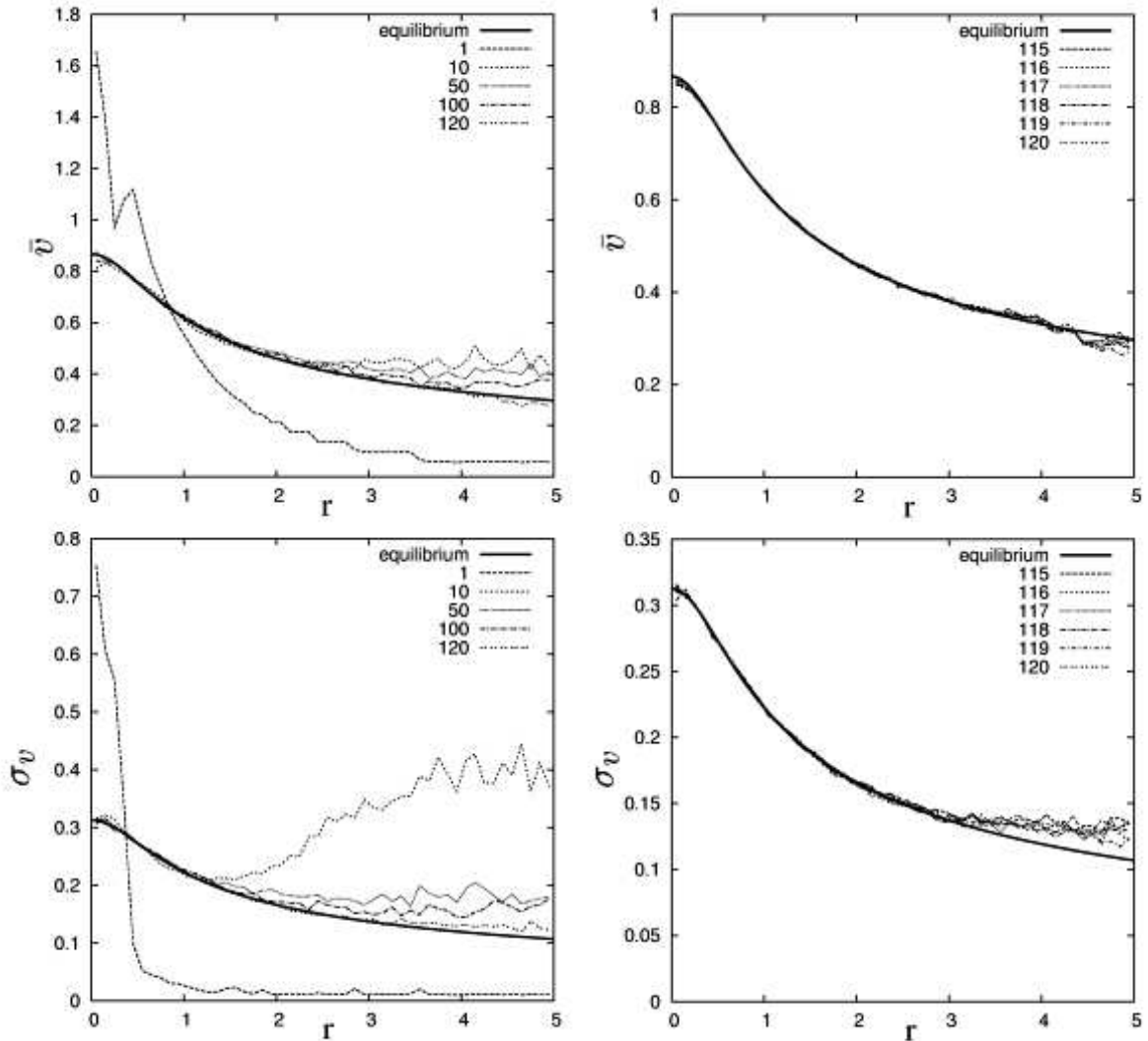


Figure 3: Convergence of iterations in the construction of model li. The upper plots show the dependence of the mean speed,  $\bar{v}$ , on  $r$ , while the lower plots show the dependence of the dispersion of the speed,  $\sigma_v$ , on  $r$  for several iterations. The left-hand plots show these quantities for the 1st, 10th, 50th, 100th, and 120th iterations, while the right-hand plots correspond to the last five iterations. The solid bold curve shows  $\bar{v}$  and  $\sigma_v$  for equilibrium model (5) (these quantities can be computed by integrating the equilibrium distribution function).

particles. We estimated this noise level by computing the average value of  $\Delta_r$  for a large number of pairs (200) of random realizations of the model at the initial time.

We computed  $\Delta_v$  in the same way, but for the distribution of particles in velocity space. For the results reported here, the width of the layer and maximum velocity were 0.1 and 1.5, respectively.

Figure 4 shows the time dependences of  $\Delta_r$  and  $\Delta_v$  for our four models. It is obvious that the values of  $\Delta_r$  and  $\Delta_v$  for models DF, li, and epol are close to their natural noise levels. At the same time, the  $\Delta_r$  value for the gauss model appreciably exceeds the noise level;  $\Delta_v$  also appreciably exceeds the noise level, although we note that the gauss model adjusts to the equilibrium state in about 15-20 time units (which approximately correspond to the crossing time for the entire system), and this regime has virtually the same profile in the equilibrium state and at the initial time.

We can draw the following general conclusion. The models constructed using the iterative method (li and epol) are essentially in equilibrium. They conserve their parameters as well as the model constructed using an equilibrium distribution function (model DF). The iterative models behave much better than the model constructed in the approximation of a Gaussian velocity distribution (model gauss).

Our models exhibit deviations from equilibrium at the very edge of the system, at  $r > 3$  (as we would expect; Fig. 3). On the whole, these models are very close to equilibrium. We emphasize again that we used cold models, which are very far from equilibrium, as the initial models for our iterations. However, through the iterations, these models came to virtually equilibrium states. Thus, the iterative approach has fully validated itself. In the next section, we apply this approach to more complex systems.

## 4.2 Equilibrium models of stellar disks

### 4.2.1 Implementation of the iterative method to construct an equilibrium model for a stellar disk

Let us apply the iterative method described above to construct an equilibrium ( $N$ -body) model for a stellar disk with a density distribution  $\rho_{\text{disk}}(R, z)$  embedded in an external potential  $\Phi_{\text{ext}}(R, z)$ . We would expect a family of equilibrium disks to exist for a given  $\rho_{\text{disk}}$  and  $\Phi_{\text{ext}}$ . This must be at least a one-parameter family characterized by the fraction of kinetic energy contained in random motions. This is where the construction of an equilibrium stellar disk differs from the construction of an equilibrium isotropic Plummer sphere – we must construct an entire family and not just one model.

The main difficulty in the iterative method is how to transfer the velocity distribution function (step 3 – see the beginning of Section 4). This is done using the moments of the distribution function and certain assumptions about the form of the velocity distribution function (here, we have some similarity to the Hernquist method). We did this as follows.

We took the disk model from which we planned to “copy” the velocity distribution function (a slightly evolved model from the previous iteration step). We then subdivided the model into concentric cylindrical layers of infinite length along the  $z$  axis. We computed in each layer the four moments of the distribution function  $\bar{v}_\varphi$ ,  $\sigma_R$ ,  $\sigma_\varphi$ , and  $\sigma_z$ , and used these moments to specify the velocities in the model for the next iteration step. We

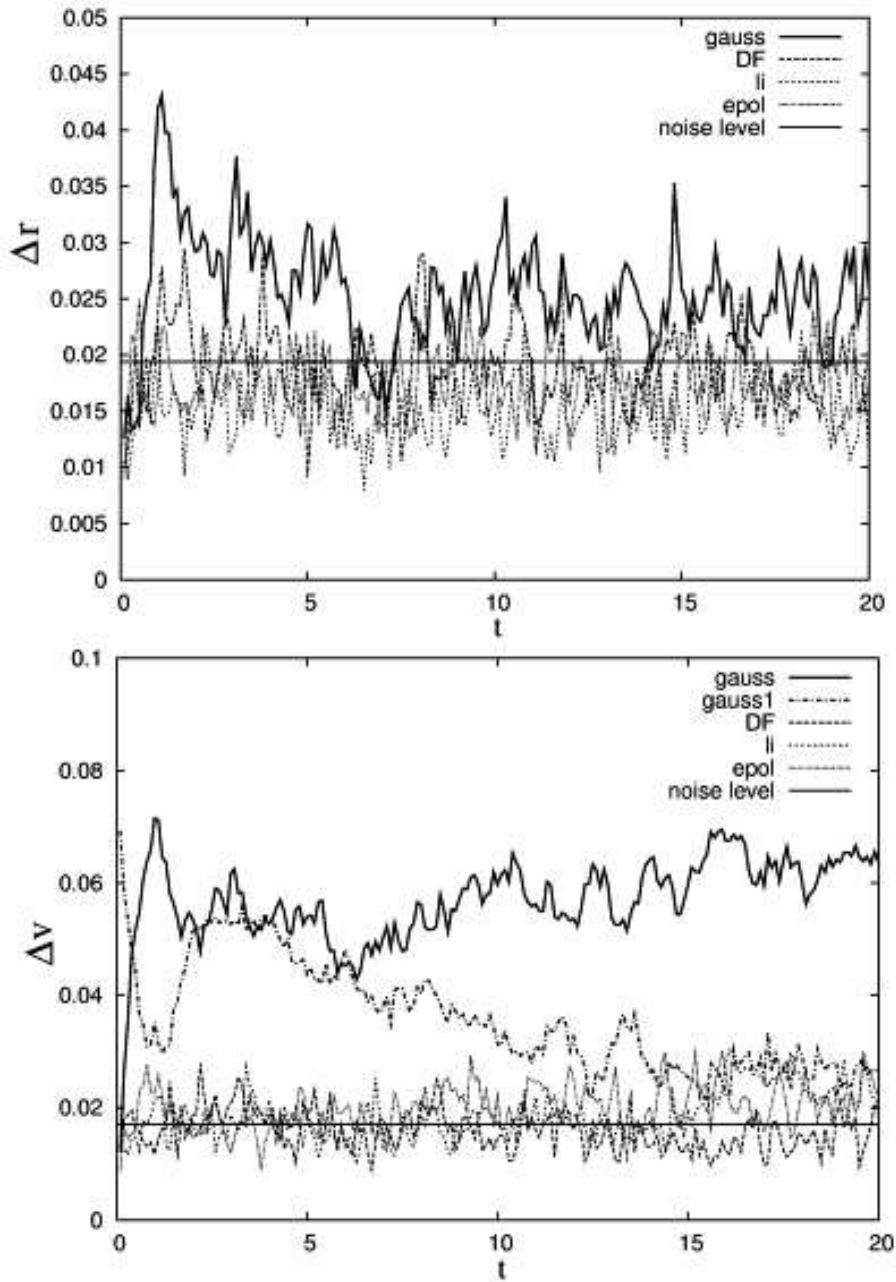


Figure 4: Time dependences of  $\Delta_r$  and  $\Delta_v$  for four  $N$ -body models of the Plummer sphere. The horizontal line shows the noise level for  $\Delta_r$  and  $\Delta_v$ . The initial distribution for the gauss model is far from equilibrium (e.g., from the velocity distribution in the DF model). We therefore computed  $\Delta_v$  for the gauss model in two different ways: first, as for all the other models, by calculating the difference between the velocity distributions at the initial time and at time  $t$  (the curve “gauss”), and second, by calculating the difference between the velocity distribution at time  $t$  and the equilibrium velocity distribution, using the initial velocity distribution for the DF model (the curve “gauss1”).

assumed that the velocity distribution has a Schwarzschild form except for one feature: we removed all particles capable of escaping beyond the disk boundary.

Let us explain this last condition. If we have specified an axisymmetric potential  $\Phi_{\text{tot}}$  (in our case  $\Phi_{\text{tot}} = \Phi_{\text{disk}} + \Phi_{\text{ext}}$ ) and a particle is specified to have the coordinates  $R, z$  and velocities  $v_R, v_\varphi, v_z$ , this particle can reach the radius  $R_{\text{max}}$  (the disk boundary) if and only if the following inequality [1](p. 117) is satisfied:

$$0.5(v_R^2 + v_z^2 + v_\varphi^2) + \Phi_{\text{tot}}(R, z) \geq \Phi_{\text{tot}}(R_{\text{max}}, 0) + \frac{v_\varphi^2 R^2}{2R_{\text{max}}^2}. \quad (6)$$

We then searched for the parameters of this so “truncated” Schwarzschild distribution ( $\bar{v}'_\varphi, \sigma'_R, \sigma'_\varphi, \sigma'_z$ ), that make its moments equal to the specified values ( $\bar{v}_\varphi, \sigma_R, \sigma_\varphi, \sigma_z$ ). In some cases, this is impossible in the peripheral regions of the galaxy. We then used in these regions an “energy-truncated” Schwarzschild distribution instead of the radius-truncated distribution, i.e., we used the Schwarzschild distribution without particles with positive total energies (particles capable of escaping to infinity).

This yields a velocity distribution function in each cylindrical layer, thereby solving the problem of transferring the velocity distribution function. Another technical point is the following. In each cylindrical layer, we have a distribution function with the parameters  $\bar{v}'_\varphi, \sigma'_R, \sigma'_\varphi, \sigma'_z$ . We referenced the value of each of these parameters to the value at the midpoint of the cylindrical layer and interpolated them using piecewise-linear functions to obtain a velocity distribution function that is continuous in radius.

We adopted the following important simplifying assumptions during the transfer of the velocity distribution function (that may fail in real stellar disks of spiral galaxies):

- the disk is isothermal in the  $z$  direction;
- by adopting the Schwarzschild velocity distribution, we implicitly assume that  $\overline{v_R v_z} = 0$ .

We wish to emphasize two important points. First, the particular implementation of the iterative method used does not matter – it is the idea behind the method that is important. Second, the main test of any method for constructing an equilibrium  $N$ -body model should, naturally, be experimentally verifying the extent to which the model is close to equilibrium.

We used the following model versions as initial models for the iterations.

- Models constructed using the Hernquist technique (see Section 2).
- Cold models in which the particles move in strictly circular orbits. This model is theoretically in equilibrium, but is highly unstable, even on time scales of the order of the iteration time. Therefore, this model becomes slightly heated in the iteration process.
- A “shifted” model. Let us assume that we have an equilibrium disk model constructed using the iterative method. In our technique, this model is determined by the four moments of the velocity distribution function in each cylindrical layer

$(\bar{v}_\varphi, \sigma_R, \sigma_\varphi, \sigma_z)$ . We construct a new model with  $\bar{v}'_\varphi = c\bar{v}_\varphi$ ,  $\sigma'_R = \frac{1}{c}\sigma_R$ ,  $\sigma'_\varphi = \frac{1}{c}\sigma_\varphi$ ,  $\sigma'_z = \sigma_z$ , where  $c$  is the shift coefficient, which is close to unity, the primed moments refer to the shifted model, and the unprimed moments refer to the old, unshifted model.

- Other versions. For example, a model constructed for a different external potential or for a disk with other parameters.

The iterations for all these versions converged and yielded various models. However, as expected, all these models form a one-parameter family (Figs. 5 and 6; see below for a more detailed description of these models).

Before starting our discussion of the properties of the iterative models, let us point out a few technical details. We must usually construct either several models in a family with the same  $\rho_{\text{disk}}$  and  $\Phi_{\text{ext}}$  or some particular model of this family. One example might be a model with a given kinetic energy fraction contained in the random motions of stars (in this case, we can fix the Toomre parameter at some radius). The convergence of the iterations is faster the closer the initial disk is to equilibrium. Therefore, to save CPU time, it is advisable to use the following “tricks.” We can initially perform the iterations with lower accuracy (fewer particles and a coarser dividing of the model into cylindrical layers during the transfer of the particle velocity distribution), and then carry out several iterations with higher accuracy. If we have already constructed one equilibrium model from a family, all the other models of this family can conveniently be constructed using shifted models (described above, where we enumerated possible initial models for the iterations). Such shifted models turn out to be much closer to equilibrium than, for example, models constructed using the Hernquist technique, and the iterations converge appreciably faster.

To accelerate the convergence of the iterations and construct models with a fixed fraction of their kinetic energy contained in random motions, we can fix this energy fraction at each iteration (i.e., fix the degree of heating of the model). Instead of fixing the amount of energy contained in random motions, we can fix the amount of energy contained in regular motions. We fixed this latter quantity via the total angular momentum with respect to the  $z$  axis:

$$L_z = \sum_{i=1}^N m_i v_{\varphi i} R_i, \quad (7)$$

where  $m_i$ ,  $v_{\varphi i}$ , and  $R_i$  are the mass, azimuthal velocity, and cylindrical radius of the  $i$ th particle, respectively.

We fixed  $L_z$  and, at each iteration step, having constructed the new model (with the same velocity distribution as in the slightly evolved model of the previous iteration step), we adjusted the azimuthal velocities of the particles to make the total angular momentum of the system exactly equal to the given  $L_z$ . We did this as follows. Let  $L_z$  be the given angular momentum and  $L'_z$ , the current angular momentum. We specified the new azimuthal velocities of the particles using the relations

$$v_{\varphi i} = v'_{\varphi i} + \frac{(L_z - L'_z)}{R_i m_i} \frac{w_i}{\sum_{j=1}^N w_j}, \quad (8)$$

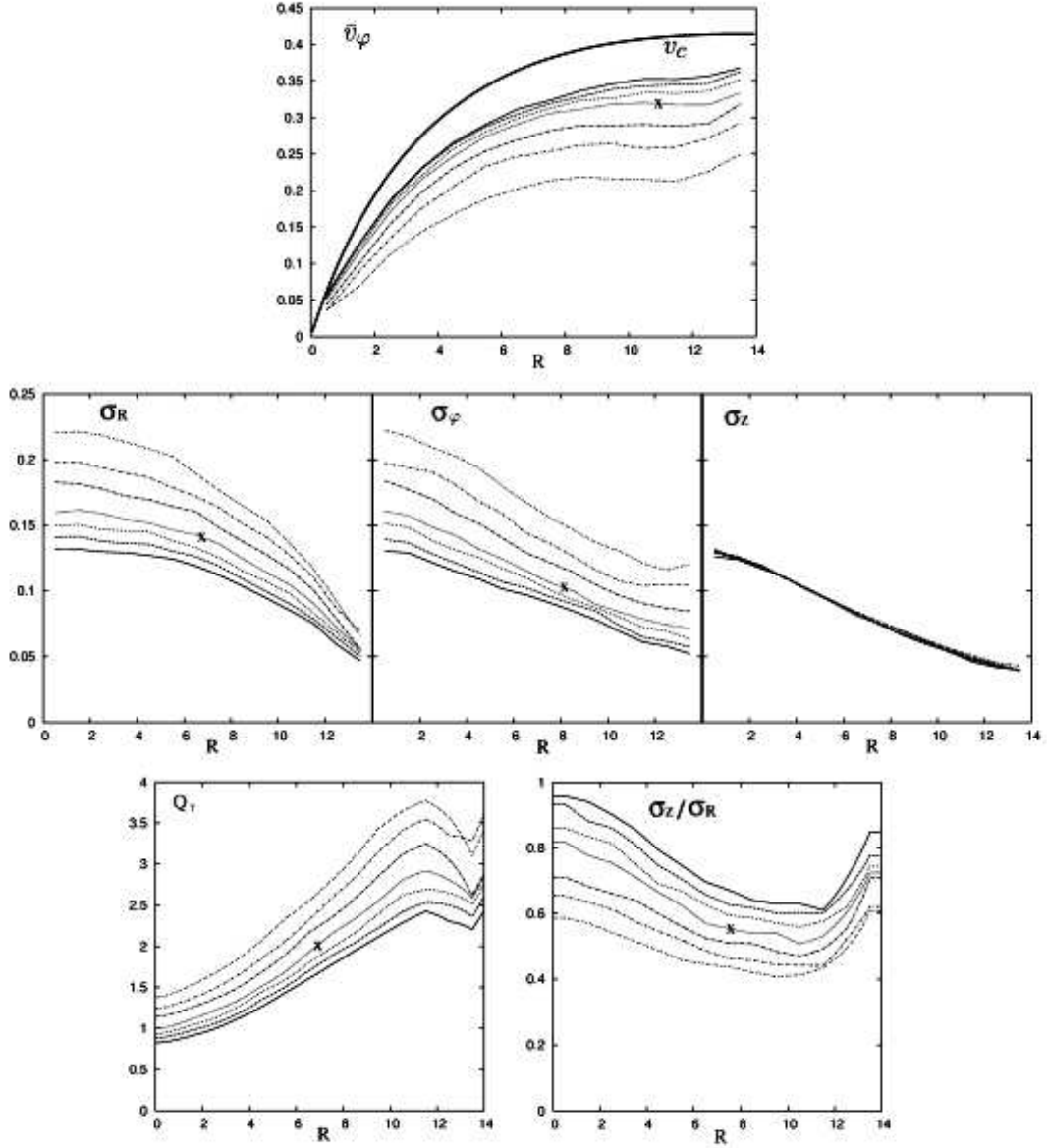


Figure 5: First family of models constructed using the iterative method. Dependences on cylindrical radius  $R$  are shown for four moments of the velocity distribution ( $\bar{v}_\varphi$ ,  $\sigma_R$ ,  $\sigma_\varphi$ , and  $\sigma_z$ ; two top rows), and the Toomre parameter  $Q_T$  and ratio  $\sigma_z/\sigma_R$  (bottom row). The cross indicates the model whose equilibrium test is shown in Fig. 9. The various curves in the plots correspond to various models in this family.

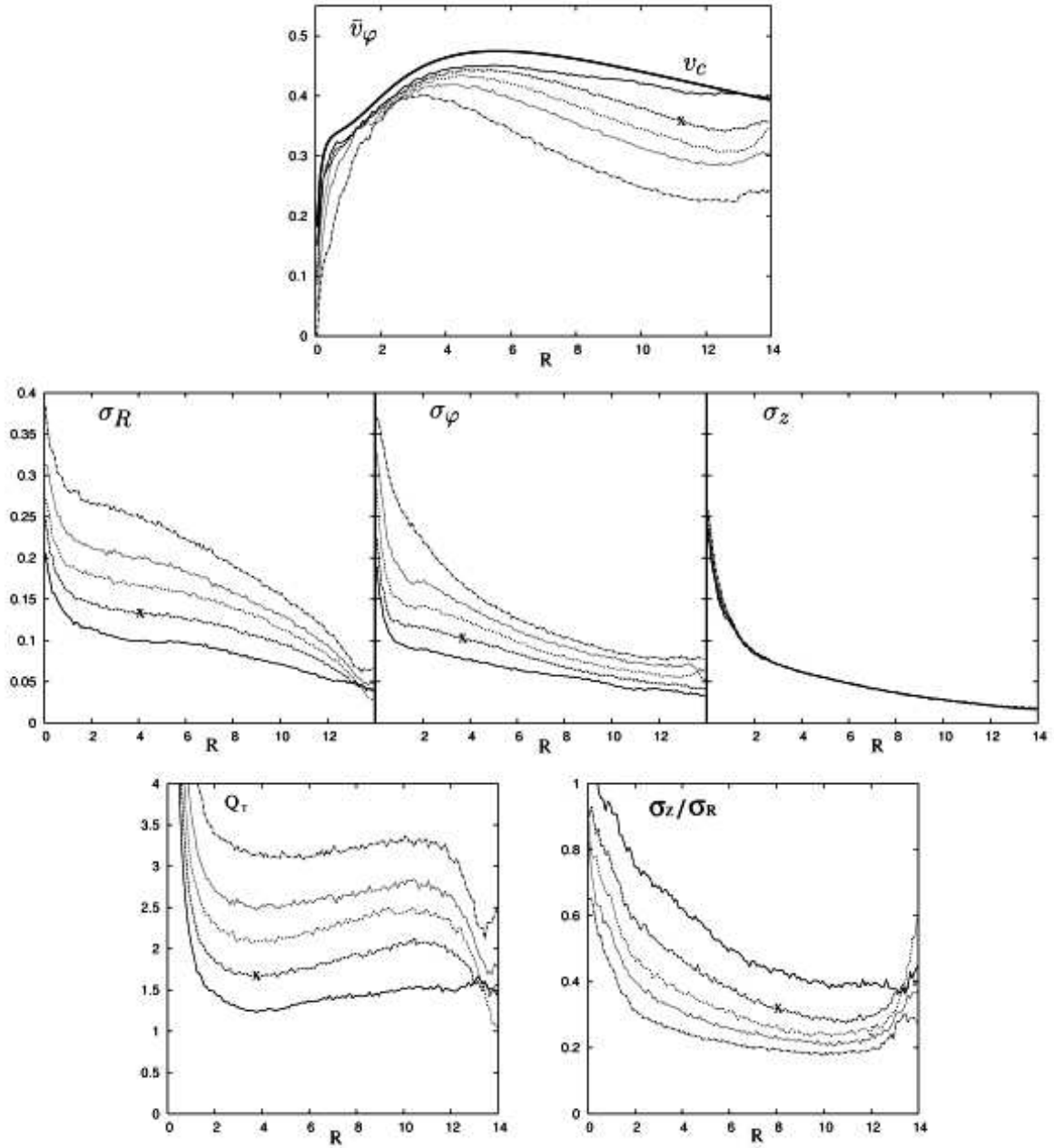


Figure 6: Same as Fig. 5 for the second family of models. The cross indicates the model whose equilibrium test is shown in Fig. 10.

where  $v'_{\varphi i}$  is the current azimuthal velocity of the  $i$ th particle,  $v_{\varphi i}$  the adjusted azimuthal velocity of this particle, and  $w_i$  a weight that determines how we add the angular momentum to the particle. In our experiments, we set  $w_i = R_i m_i$ .

Iterations with fixed  $L_z$  converged to models of the same family as the iterations without fixed  $L_z$ . However, the iterations with fixed  $L_z$  converged much faster. Fixing  $L_z$  is helpful, since it results in the convergence of the iterations to a strictly defined model from a family of iterative models with given  $\rho_{\text{disk}}$  and  $\Phi_{\text{ext}}$ , irrespective of the initial model.

#### 4.2.2 Properties of the iterative disk models

Let us consider as examples two families of models constructed using the iterative method.

Figure 5 shows the first family. We adopted disk model (2) with  $h = 3.5$ ,  $z_0 = 1$ ,  $M_{\text{disk}} = 1$ , and  $R_{\text{max}} = 14$ , and modeled the external potential using the Plummer sphere (4) with  $a_{\text{pl}} = 15$  and  $M_{\text{pl}} = 4$ . For these parameters, the fractional mass of the spherical subsystem within four exponential radii is equal to about 1.3 (i.e.,  $M_{\text{sph}}(4h)/M_{\text{disk}}(4h) \approx 1.3$ ). Note that the parameters of the disk and external potential are the same as in the model constructed using the Hernquist technique (Fig. 1), which was used as an example of a not-quite-equilibrium model. The time for a single iteration,  $t_i = 15$ , corresponds to approximately one-tenth of a disk rotation at a distance of two exponential disk scales. The thickness of the cylindrical layers into which we subdivided the model when transferring the velocity distribution function is  $d_R = 1$ . We used  $N = 10^5$  particles.

Figure 6 shows the second family. It was produced using an initially thinner disk model (2) with  $h = 3.5$ ,  $z_0 = 0.3$ ,  $M_{\text{disk}} = 1$ , and  $R_{\text{max}} = 14$ , modeling the external potential using the Plummer sphere (4) with  $a_{\text{pl}} = 3.5$ ,  $M_{\text{pl}} = 0.88$  and the potential of a Hernquist [35] sphere

$$\Phi(r) = -\frac{GM_{\text{hr}}}{r + a_{\text{hr}}}, \quad (9)$$

with  $a_{\text{hr}} = 0.5$  and  $M_{\text{hr}} = 0.2$ . In this case, the Plummer and Hernquist spheres play the role of a dark halo and bulge, respectively. The total relative mass of the spherical subsystem within four exponential disk parameters is approximately unity ( $M_{\text{sph}}(4h)/M_{\text{disk}}(4h) \approx 1$ ). The duration of a single iteration is  $t_i = 15$ ; the thickness of the cylindrical layers into which we subdivided the model for the transfer of the velocity distribution function is  $d_R = 0.1$  (i.e., a less coarse dividing than in the first case), and the number of particles is  $N = 5 \cdot 10^5$ .

The models constructed using the iterative method have the following properties.

1. The models prove to be close to equilibrium. They preserve both their structural and dynamical parameters well during the initial stages of their evolution (Figs. 9 and 10). It goes without saying that different values of  $\rho_{\text{disk}}$  and  $\Phi_{\text{ext}}$  yield models with different degrees of closeness to equilibrium. For example, the models of a thin stellar disk without an external potential (with the density distribution (2) and  $h = 3.5$ ,  $z_0 = 0.3$ ,  $M_d = 1$ ,  $R_{\text{max}} = 14$ ) are appreciably nonequilibrium. However, in any case, the resulting models are substantially closer to equilibrium than those constructed using the Hernquist technique (see Section 2). We consider possible reasons for deviations of the iterative models from equilibrium below.

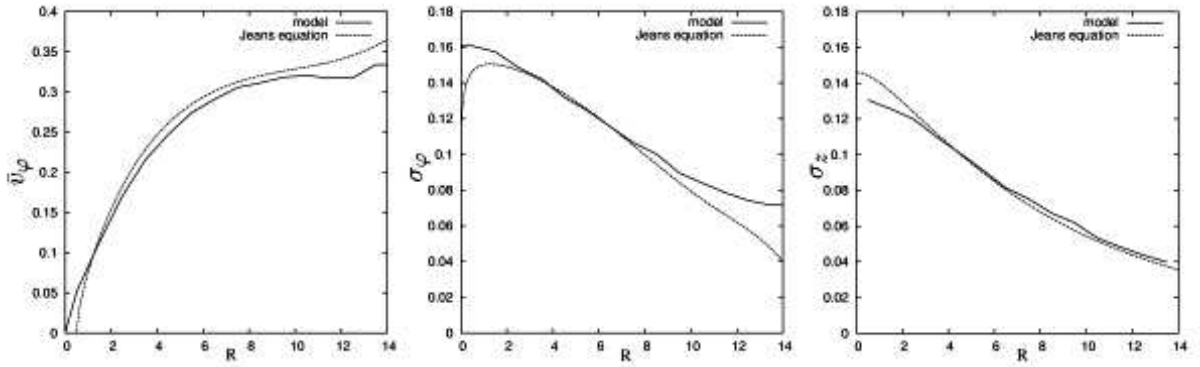


Figure 7: Comparison of the moments of the velocity distribution function for the iterative model of the first family with the solutions of the Jeans equations (1). In the left-hand plot, the solid curve (model) shows the mean azimuthal velocity for the iterative model, and the dashed curve (Jeans equation) shows the same quantity computed proceeding from the Jeans equation [the first equation of (1)], where we adopted  $\sigma_R$  and  $\sigma_\varphi$  from the iterative model. In the middle plot, the solid curve shows the azimuthal velocity dispersion for the iterative model, and the dashed curve the same quantity computed using the Jeans equations [the second equation of (1)], where we adopted  $\bar{v}_\varphi$  and  $\sigma_R$  from the iterative model. In the right-hand plot, the solid curve shows the dispersion of the stellar velocities in the vertical direction, and the dashed curve the same quantity computed using the Jeans equations [the third equation of (1)]. We used a model of the family presented in Fig. 5 (marked by a cross).

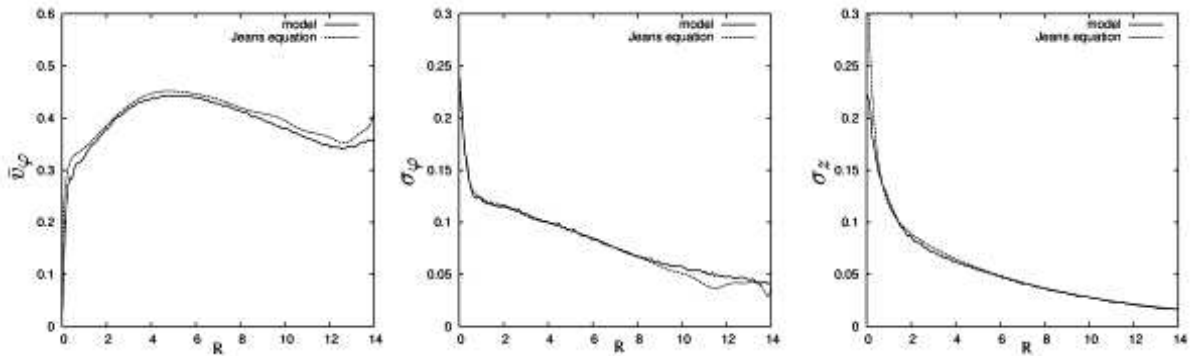


Figure 8: Same as Fig. 7 for the iterative model of the second family. We used a model of the family shown in Fig. 6 (marked by a cross).

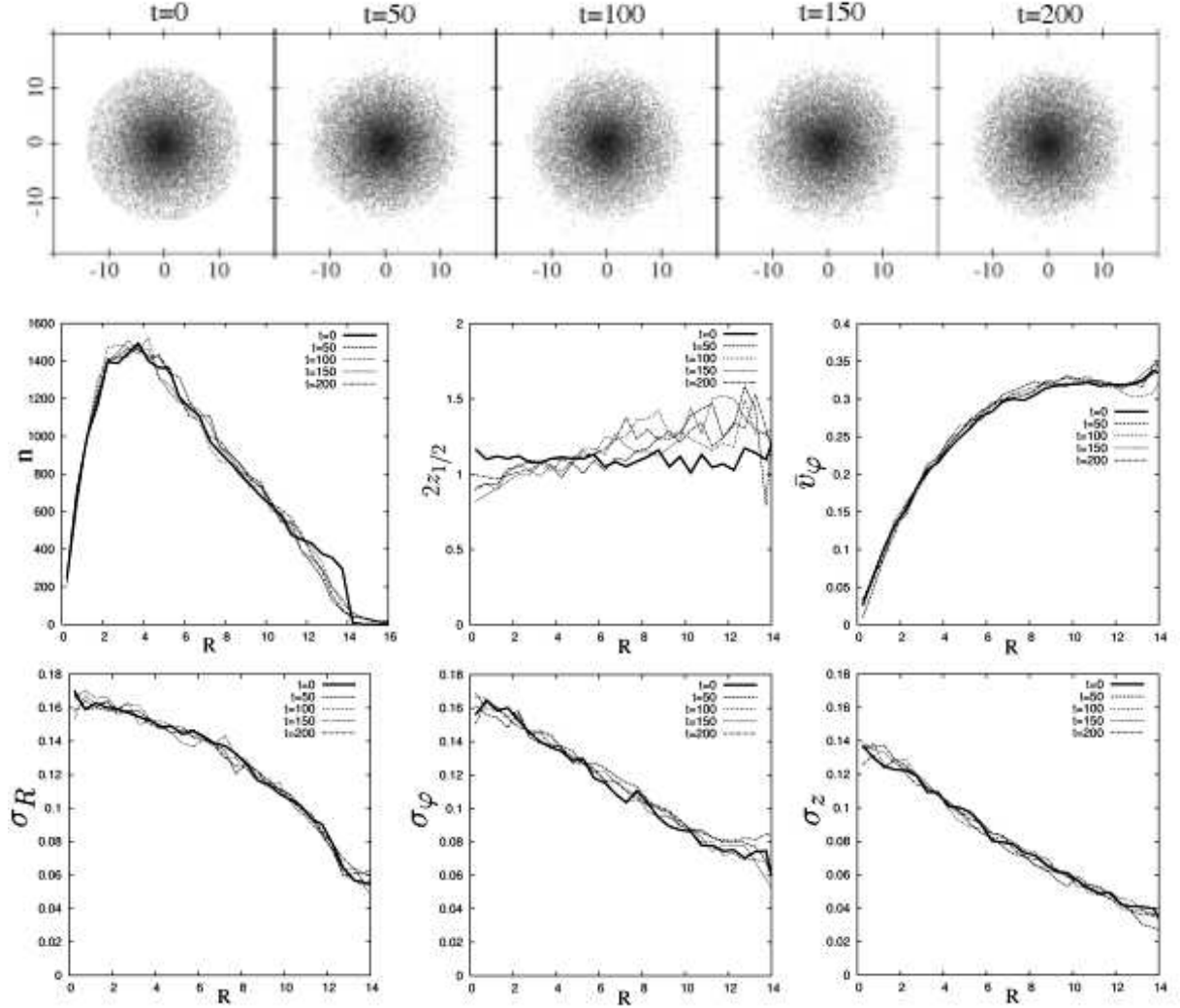


Figure 9: Initial stages of the evolution of an iterative model in the first family. A model of the family shown in Fig. 5 (marked by a cross) is used. The top snapshots show a face-on view for several times, with the shades of gray corresponding to the logarithm of the particle number per pixel. The plots in the central and bottom parts of the figure show the dependences of various disk parameters on the cylindrical radius  $R$  for various times: the number of particles in concentric cylindrical layers  $n$ , twice the median of  $|z|$ ,  $2z_{1/2}$  (which characterizes the disk thickness and is close to  $z_0$  for the distribution (2)), and the four moments of the velocity distribution function  $\bar{v}_\varphi$ ,  $\sigma_R$ ,  $\sigma_\varphi$ , and  $\sigma_z$ .  $N = 25\,000$ ,  $\epsilon = 0.02$ , and  $dt = 0.01$ . The disk thickness can be seen to have changed slightly. This is probably due to the assumption that the  $z$ -velocity distribution function is isothermal.

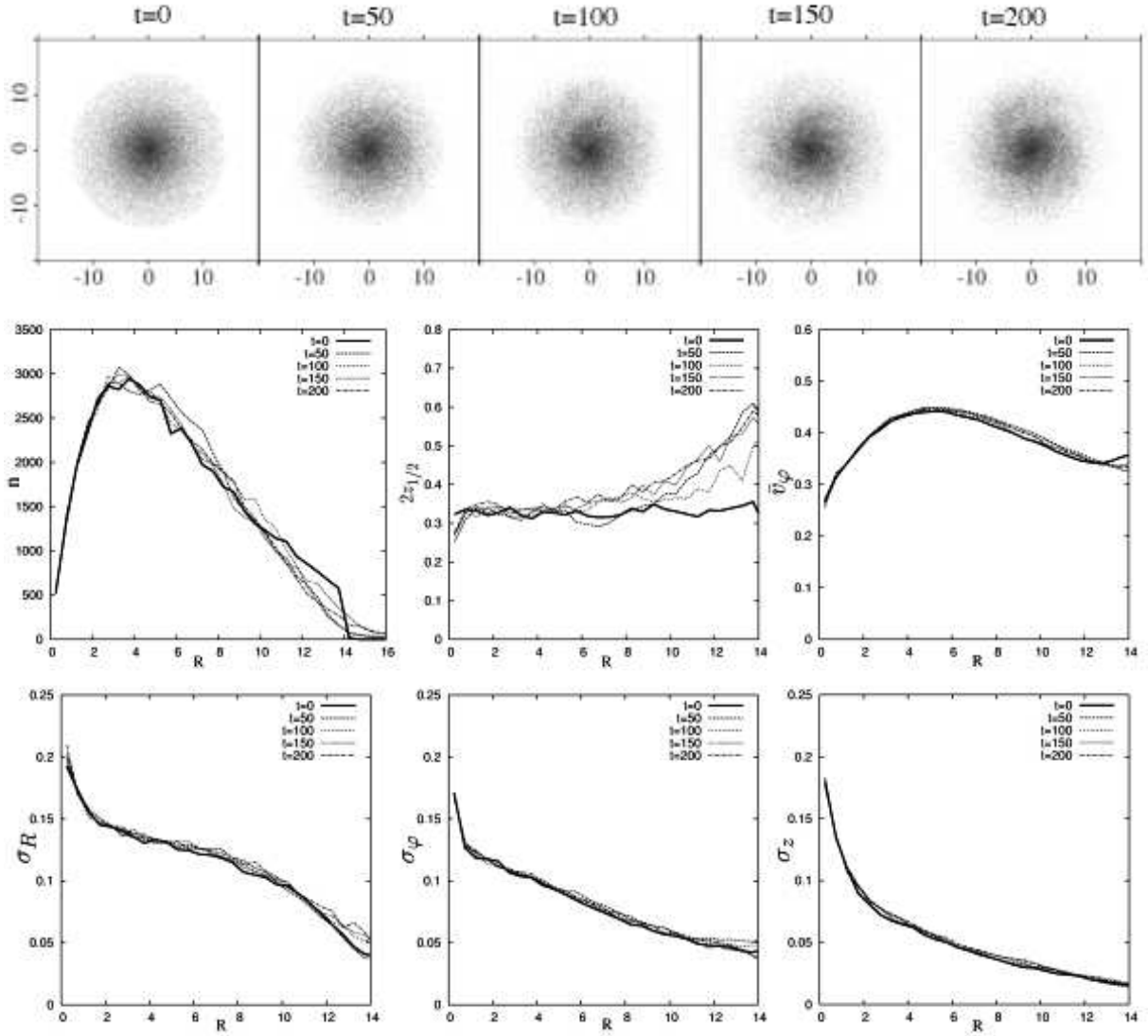


Figure 10: Same as Fig. 9 for an iterative model of the second family ( $N = 50000$ ,  $\epsilon = 0.02$ ,  $dt = 0.01$ ). A model of the family shown in Fig. 6 (marked by a cross) is used.

2. The first four moments of the velocity distribution function fairly accurately obey the equilibrium Jeans equations (1) (Figs. 7 and 8). This means that, if we replaced the assumed dependence  $\sigma_R(R)$  in the Hernquist method (see Section 2) with the dependence obtained from the iterations, the resulting models will be very similar to the iterative models, i.e., they essentially be in equilibrium. In other words, given a more correct assumption about the dependence  $\sigma_R(R)$ , the Hernquist technique would allow the construction of close-to-equilibrium models.
3. All models in some family of iterative models have the same vertical-velocity dispersion profile  $\sigma_z(R)$  (Figs. 5 and 6). This means that the equilibrium condition in the vertical direction is completely decoupled from the disk equilibrium condition in the plane. This was expected, since, of all the moments of the velocity distribution function, only  $\sigma_z$  appears in the Jeans equation describing equilibrium in the vertical direction [the last equation of (1)].
4. The profile of the radial stellar-velocity dispersion,  $\sigma_R$ , differs strongly from the commonly adopted exponential profile (Figs. 5 and 6).

### 4.2.3 Specific features of the iterative disk models. Further development of the technique

Let us now turn to some specific features of our iterative models.

1. Our stellar disk model (2) is not a very good choice. The density profile in this model has a sharp cutoff. Naturally, such a structure cannot be in equilibrium, and the disk must have a smooth cutoff. We can see in Figs. 9 and 10 (the left-hand plot in the middle row) how this sharp cutoff is disrupted. We conclude that we must choose an initial stellar-disk model with a smooth density decrease at  $R$  values close to  $R_{\max}$ .
2. As is clear from Figs. 9 and 10 (middle plot in the middle row), the thickness of the stellar disk varies somewhat during the initial stages of evolution. These variations can be seen in almost all the iterative models, and are more pronounced in models that are hotter in the disk plane and less pronounced in models that are cooler in the disk plane (here, hotter means that a higher fraction of the kinetic energy is contained in random motions). This nonequilibrium state of the iterative models is likely due to the assumptions about the velocity distribution function adopted when implementing our method, in particular our assumption that the velocity distribution function does not depend on  $z$  (the model is isothermal in the  $z$  direction). In addition, the assumption that  $\overline{v_R v_z} = 0$  may not be valid in the central regions. Future analyses should apply the iterative method without these assumptions, first and foremost, without the isothermal assumption, especially since this method is easy to generalize in this way. In the technique described here, we subdivided the model into cylindrical layers when transferring the velocity distribution function from the previous iteration step. Each of these cylindrical layers can be subdivided into layers along the  $z$  axis, and the moments of the

velocity distribution function can be computed separately in each layer (i.e., the model can be subdivided in both the  $R$  and  $z$  planes). Note, however, that such a modification of the iterative method requires a far greater number of particles than we have used so far.

3. The iterative method cannot yield an equilibrium model that is unstable on time scales shorter than the time for one iteration. For example, the method cannot produce a very cold model. As is evident in Figs. 5 and 6, the family of iterative models is bounded on the side of cold models. It is not possible to construct a very cold model, even when  $L_z$  is fixed – the iterations still fail to converge.

#### 4.2.4 Assumption of uniqueness of the family of models. New applications for iterative models

Thus, the technique described above can be used to construct a one-parameter family of close-to-equilibrium models for a given  $\rho_{\text{disk}}$  and  $\Phi_{\text{ext}}$ . This family is parametrized by the fraction of kinetic energy contained in random motions (e.g., this parameter can have the form of the total angular momentum of the disk with respect to the  $z$  axis,  $L_z$ ). The question naturally arises in this case of whether there are other equilibrium models besides those in the family of iterative disk models? We can only postulate that there can be only one equilibrium disk model. Such a hypothesis can be formulated follows. There can be at most one equilibrium model (one equilibrium distribution function) for a given  $\rho_{\text{disk}}(R, z)$ ,  $\Phi_{\text{ext}}(R, z)$  with a fixed fraction of kinetic energy contained in random motions (e.g., for fixed  $L_z$ ).

We can neither prove nor disprove this statement, and can only assume that it is true. This assumption expands the scope of application of the iterative models. We can compare iterative models to observational data in order to derive constraints on unobserved parameters of galaxies. For example, our statement that the dependence of  $\sigma_R$  on  $R$  for the iterative models is far from exponential requires additional explanations. More precisely, this dependence is far from exponential for the  $\rho_{\text{disk}}$  and  $\Phi_{\text{ext}}$  considered. It is not ruled out that an external potential can be selected so as to make the dependence of  $\sigma_R$  on  $R$  exponential [8] (see also Section 3, where we discuss the observational data for this dependence). When available, GAIA data on the velocity field in our Galaxy can be used to try to constrain the mass distribution in the dark halo of the Galaxy via iterative models (by selecting an external potential that makes the equilibrium stellar disk embedded in this potential have the observed velocity field).

## 5 Conclusions

We have proposed here a new iterative approach to constructing equilibrium  $N$ -body models with a given density distribution. The main idea of this approach is the following. At the first stage, a model is constructed using some approximate method. The model is then allowed to adjust to the equilibrium state while its density distribution is kept fixed, as well as the required parameters of the velocity distribution, if necessary.

We used our iterative approach to construct two types of models. The first type have the form of isotropic and spherically symmetric systems. We used the iterative approach to construct such systems in order to test whether the approach indeed enables the construction of close-to-equilibrium models. The second type of models were axisymmetric stellar disks in an external potential. In both cases, the numerical models constructed using the iterative approach were very close to equilibrium. The iterative models for the stellar disks were much closer to equilibrium than models constructed based on the Jeans equations (see Section 2).

We also show that the hypothesis that the radial velocity dispersion is proportional to the vertical velocity dispersion in spiral galaxies ( $\sigma_R \propto \sigma_z$ ) may be incorrect. First, this assumption lacks clear observational evidence to support it. Second, it is not true for the iterative models of stellar disks that we have constructed. Finally, the assumption that  $\sigma_R \propto \sigma_z$  is the main reason why the stellar disks constructed using the technique of Hernquist [9] are fairly far from equilibrium. To prove this last statement, recall that, since the iterative models of stellar disks obey the Jeans equations, if we replace in Hernquist's technique the relation  $\sigma_R \propto \sigma_z$  with the dependence  $\sigma_R(R) = \sigma_R^i(R)$ , where  $\sigma_R^i(R)$  is the radial dispersion profile for an iterative model, the resulting models should be as close to equilibrium as the iterative models.

The proposed method has a wide range of applications, and can be used to construct models with various geometries. For example, it can be used to construct spherically symmetric models with anisotropic stellar motions, as well as self-consistent multicomponent models of disk galaxies. Unlike the kinetic approach based on the distribution function, our method provides direct input data for  $N$ -body simulations.

Furthermore, the proposed method has purely astrophysical applications. For example, bringing the velocity field obtained in equilibrium iterative models into agreement with the velocity field in our Galaxy can enable determination of the parameters of the external potential, and, consequently, the dark halo.

## Acknowledgment

This work was supported by the Russian Foundation for Basic Research (project codes 03-12-17152 and 06-02-16459) and the Program of Support for Leading Scientific Schools of the Russian Federation (grant NSh-8542.2006.2).

## References

- [1] J. Binney and S. Tremaine, *Galactic Dynamics*, Princeton University Press, 1987
- [2] J.F. Navarro, C.S. Frenk, and S.D.M. White, *Astrophys. J.* **462**, 563(1996)
- [3] L.M. Widrow, *Astrophys. J. Suppl.* **131**, 39(2000)
- [4] E.L. Lokas and G.A. Mamon, *MNRAS* **321**, 155(2001)
- [5] A.J. Kalnajs, *Astrophys. J.* **175**, 63(1972)

- [6] W. Dehnen and J.J. Binney, MNRAS **298**, 387(1998)
- [7] K. Kuijken and J. Dubinski, MNRAS **277**, 1341(1995)
- [8] L.M. Widrow and J. Dubinski, Astrophys. J. **631**, 838(2005)
- [9] L. Hernquist, Astron. Astrophys. Suppl. Ser. **86**, 389(1993)
- [10] I.R. King, *Vvedenie v klassicheskuyu zvezdnuyu dinamiku (An Introduction to Classical Stellar Dynamics)* (URSS, Moscow, 2002) [in Russian]
- [11] Y. Revaz and D. Pfenniger, Astron. Astrophys. **425**, 67(2004)
- [12] A. V. Khoperskov, A. V. Zasov, and N. V. Tyurina, Astron. Zh. **80**, 387(2003) [Astron. Rep. **47**, 357 (2003), astro-ph/0306198]
- [13] E. Athanassoula and A. Misiriotis, MNRAS **330**, 35(2002)
- [14] N.Ya. Sotnikova and S.A. Rodionov, Pis'ma Astron. Zh. **29**, 367(2003) [Astron. Lett. **29**, 321 (2003), astro-ph/0304215]
- [15] N.Ya. Sotnikova and S.A. Rodionov, Pis'ma Astron. Zh. **31**, 17 (2005) [Astron. Lett. **31**, 15 (2005), astro-ph/0412063]
- [16] P.C. van der Kruit and L. Searle, Astron. Astrophys. J, **95**, 105(1981)
- [17] L. Spitzer, Astrophys. J. **95**, 325(1942)
- [18] A. Toomre, Astrophys. J. **139**, 1217(1964)
- [19] J. Lewis and K.C. Freeman, Astron. J. **97**, 139(1989)
- [20] N.V. Tyurina, Candidate's Dissertation in Mathematics and Physics (Mosk. Gos. Univ., Moscow, 2002).
- [21] R. Bottema, Astron. Astrophys. **275**, 16(1993)
- [22] J. Bahcall, Astrophys. J. **276**, 156(1984)
- [23] P. Amendt and Ph. Cuddeford, Astrophys. J. **368**, 79(1991)
- [24] Ph. Cuddeford and P. Amendt, MNRAS **253**, 427(1991)
- [25] M. Kregel and P.C. van der Kruit, MNRAS **358**, 481(2005)
- [26] J. Gerssen, K. Kuijken and M.R. Merrifield, MNRAS **317**, 545(2000)
- [27] J. Gerssen, K. Kuijken and M.R. Merrifield, MNRAS **288**, 618(1997)
- [28] K.L. Spapiro, J. Gerssen and R.P. van der Marel, Astron. J. **126**, 2707(2003)
- [29] K.B. Wesfall, M.A. Barshady, M.A.W. Verheijen, et al., astro-ph/0508552

- [30] O. Bienaymé and N. Séchaud, *Astron. Astrophys* **323**, 781(1997)
- [31] R. Fux and L. Martinet, *Astron. Astrophys.* **287**, 21(1994)
- [32] J.A. Sellwood and E. Athanassoula, *MNRAS* **221**, 195(1986)
- [33] J. Barnes, *Astrophys. J.* **331**, 699(1988)
- [34] S.A. Rodionov and N.Ya. Sotnikova, *Astron. Zh.* **82**, 527 (2005) [*Astron. Rep.* **49**, 470 (2005), astro-ph/0504573]
- [35] L. Hernquist, *Astrophys. J.* **356**, 359(1990).

Translated by A. Dambis